International Journal of Nanomedicine

Dovepress
Taylor & Francis Group

Open Access Full Text Article

ORIGINAL RESEARCH

Exosomal THBS4 Derived From Human Placental Mesenchymal Stem Cells Promotes the Migration and Angiogenesis of the Endothelial Cells in Preeclampsia by Activating the Integrin α2/PI3K/AKT Axis

Zejun Yang[1,*], Yu Liu[1,2,*], Jianjian Cui[1,3,*], Zhirui Chen[4], Haoran Shi[1], Hui Tao[1], Ruilin Ma[1], Wencong He[1], Lei Sun[1], Yanan Li[1], Ziyang Liu[1], Zetong Wang[1], Yin Zhao[1,5]

[1]Department of Obstetrics and Gynecology, Union Hospital, Tongji Medical College, Huazhong University of Science and Technology, Wuhan, People's Republic of China; [2]Department of Obstetrics and Gynecology, West China Second University Hospital, Sichuan University, Chengdu, People's Republic of China; [3]Department of Obstetrics and Gynecology, Zhongnan Hospital, Wuhan University, Wuhan, People's Republic of China; [4]Department of Obstetrics, Maternal and Child Health Hospital of Hubei Province, Tongji Medical College, Huazhong University of Science and Technology, Wuhan, People's Republic of China; [5]Shenzhen Huazhong University of Science and Technology Research Institute, Shenzhen, People's Republic of China

*These authors contributed equally to this work

Correspondence: Yin Zhao, Department of Obstetrics and Gynecology, Union Hospital, Tongji Medical College, Huazhong University of Science and Technology, Wuhan, People's Republic of China, Email zhaoyin@hust.edu.cn

Introduction: Preeclampsia (PE) is a pregnancy-specific disease with limited treatment options. Although human placental mesenchymal stem cells (hPMSCs) hold therapeutic potential, their clinical use faces safety and practical challenges. Placental mesenchymal stem cell exosomes (PMSC-Exos) offer a promising cell-free alternative. We hypothesized that PMSC-Exos may effectively alleviate PE and investigated the underlying molecular mechanisms.

Methods: Exosomes derived from hPMSCs were isolated and characterized by transmission electron microscopy, nanoparticle tracking analysis, Western blotting (WB), and nanoparticle flow cytometry. Proteomic profiling compared PMSC and exosome protein profiles. THBS4 expression was assessed in healthy and PE placental tissues using quantitative real-time PCR, WB, and immunohistochemistry (IHC). The effects of PMSC-Exos on endothelial cells were examined by exosome uptake assay, transwell migration assay, tube formation assay, immunofluorescence, and Western blotting. In a rat PE model, PMSC-Exos were administered via intraplacental injection. Therapeutic outcomes were assessed by measuring systolic blood pressure, urinary protein levels, and analyzing placental and renal tissues with Hematoxylin and Eosin staining, IHC, and WB.

Results: We successfully isolated and characterized PMSC-Exos, which were enriched with THBS4 compared to PMSCs. THBS4 expression was downregulated in preeclamptic versus healthy placental tissues. In vitro experiments demonstrated that THBS4 contained in PMSC-Exos bound to integrin α2 (ITG α2) on endothelial cells, leading to the activation of the PI3K/AKT signaling pathway and enhanced endothelial cell migration and angiogenic function. In vivo, administration of PMSC-Exos alleviated PE symptoms, improved placental structure, and supported fetal growth.

Conclusion: These findings demonstrate that PMSC-Exos promote vascular endothelial cell migration and angiogenesis through the THBS4/integrin α2/PI3K/AKT axis, leading to improved pregnancy outcomes in a rat model of PE. THBS4 may serve as a key therapeutic target for preeclampsia. This proof-of-concept study supports the therapeutic potential of PMSC-Exos, pending further translational research.

Keywords: thrombosponding-4, mesenchymal stem cell, exosomes, endothelial cells, preeclampsia, placenta

https://doi.org/10.2147/IJN.S572708
Received: 8 October 2025
Accepted: 23 January 2026
Published: 31 January 2026

Introduction

Preeclampsia (PE) is a serious complication of pregnancy with an incidence rate of 5–7%.[1] Apart from termination of pregnancy, there are no other effective treatment options, and the perinatal outcome of patients with early-onset and severe disease is not optimistic.[2] Therefore, it is clinically imperative to develop innovative treatment approaches for preeclampsia. A promising therapeutic strategy for preeclampsia involves targeting its fundamental pathological mechanisms. Although early-onset and late-onset PE may differ in their initial triggers, both subtypes converge on a common terminal pathway: systemic endothelial dysfunction.[3] This dysfunction is primarily driven by the placental release of anti-angiogenic factors and inflammatory cytokines into the maternal circulation—a process itself rooted in abnormal placental vascular development, including inadequate spiral artery remodeling. The resulting endothelial injury leads to increased vascular permeability, vasoconstriction, and a pro-inflammatory state, which collectively manifest as the clinical hallmarks of hypertension, proteinuria, and edema.[4,5] Consequently, alleviating endothelial damage and restoring endothelial function represent critical therapeutic objectives for PE, with the potential to mitigate maternal symptoms and improve pregnancy outcomes.

Mesenchymal stem cells (MSCs), first described in 1976,[6] can be easily extracted from a range of tissues, such as adipose tissue, umbilical cord, bone marrow, and placenta.[7] As pluripotent stem cells, they possess the capacity to give rise to diverse cell types,[8] and exert immunomodulatory, tissue-reparative, and regenerative effects.[9] Early hypotheses attributed the healing capabilities of MSCs primarily to their homing ability and differentiation potential. However, more recent research increasingly suggests that paracrine signaling is a key mechanism underlying their therapeutic effects.[10] Among the key paracrine mediators are exosomes (Exos),[11] which serve as essential vehicles for RNAs, proteins, and other bioactive molecules derived from MSCs.[12] Mesenchymal stem cell exosomes (MSC-Exos) exhibit several beneficial properties compared with whole cells, such as superior stability, decreased immunogenicity, reduced lung entrapment, and an ability to traverse the placental barrier. They also present a diminished risk of complications associated with cellular therapies, including chromosomal abnormalities, tumor formation, thrombotic events, and immune-mediated rejection.[13,14] These features have sparked growing interest in MSC-Exos as potential therapeutics for preeclampsia,[15–17] cardiovascular and cerebrovascular diseases,[18] respiratory disease,[19] liver diseases,[20] inflammatory bowel disease,[21] cancer,[22] and so on. However, translating MSC-exos therapy requires careful consideration of challenges related to scalable production, standardization, source variability, and long-term safety profiles.[23]

Our preliminary studies found that placental mesenchymal stem cells engineered to overexpress heme oxygenase-1 (HO-1) enhanced angiogenesis and facilitated spiral artery remodeling in vitro through regulating the expression of angiogenic mediators[24] and improved placental vascular abnormalities, enhanced placental perfusion, alleviated symptoms of preeclampsia, and positively influenced pregnancy outcomes in a preeclampsia-like rat model.[25] Given the pivotal role of exosomes in MSC-mediated signaling and their advantages over whole-cell therapies, we hypothesized that placental mesenchymal stem cell exosomes (PMSC-Exos) may also exert therapeutic effects in PE.

In this study, we performed a comparative proteomic analysis of PMSC-Exos and their parent mesenchymal stem cells to identify potential bioactive mediators. The analysis revealed that THBS4 was significantly upregulated in PMSC-Exos compared with the originating PMSCs. Previous studies have shown that THBS4 expression is markedly decreased in placental tissues from preeclamptic pregnancies compared with normal controls. Downregulation of THBS4 has been implicated in PE pathogenesis by impairing trophoblast invasion through the TGFβ1/Smad signaling pathway.[26] These findings suggest that THBS4 may serve as a therapeutic target in PE, and its high expression in exosomes could contribute to the therapeutic potential of PMSC-Exos. We further assessed the effects of PMSC-Exos on human umbilical vein endothelial cells (HUVECs). Additionally, the therapeutic efficacy of PMSC-Exos was evaluated in a rat model of preeclampsia. To achieve targeted placental therapy and enhance local bioavailability while minimizing systemic exposure, PMSC-Exos were administered via local placental injection in our in vivo experiments.[27] However, this delivery approach presents methodological challenges, including the need for precise injection techniques, optimization of dosing regimens, and a thorough assessment of local versus systemic effects.[25] Collectively, these investigations were designed to elucidate both the functional properties and the molecular mechanisms underlying the therapeutic actions of PMSC-Exos in preeclampsia.

Methods

Isolation and Culture of PMSCs

All procedures involving human samples were conducted in accordance with protocols approved by the Ethics Review Board of Wuhan Union Hospital (approval number: 0937–01). Written informed consent was acquired from every donor before sample acquisition. The baseline clinical profiles of the study participants are summarized in Supplementary Tables 1–3. PMSCs were isolated and characterized as previously described.[24,25,28]

Cell Culture

PMSCs were cultured in DMEM/F12 medium (Gibco, USA), supplemented with 10% fetal bovine serum (Gibco, USA), at 37°C in a humidified incubator containing 5% CO_2. HUVECs, acquired from the American Type Culture Collection (ATCC, USA), were grown in endothelial cell medium (ECM) (ScienceCell, USA) with 10% fetal bovine serum (HYCEZMBIO, China) under the same conditions.

Isolation and Identification of PMSC-Exos

PMSC-Exos were extracted using ultracentrifugation. Upon reaching approximately 80% confluence, the cell culture medium was replaced with DMEM/F12, supplemented with 10% exosome-free fetal bovine serum, and incubated for an additional 48 hours. The conditioned medium was subsequently collected and subjected to sequential centrifugation: first at 300 ×g for 10 minutes to remove intact cells, followed by centrifugation at 2000 ×g for 20 minutes to eliminate cellular debris. The resulting supernatant was then concentrated using an Amicon Ultra-15 Centrifugal Filter Unit (100 kDa, Millipore, USA), subjected to centrifugation at 4000 ×g for 20 minutes. The sample was further processed with centrifugation at 10,000 ×g for 30 minutes and passed through a 0.22 μm membrane (Corning, USA). The sample was then subjected to two rounds of centrifugation at 120,000 ×g for 70 minutes. The resulting pellet was collected and resuspended in 200 μL phosphate-buffered saline (PBS). Sucrose density gradient fractionation was conducted for exosome purification.[29] The exosome pellet obtained from the initial differential ultracentrifugation was layered on top of a discontinuous sucrose density gradient (2.0 M, 1.3 M, 1.16 M, 0.8 M, and 0.5 M) followed by ultracentrifugation at 100000×g for 18 h at 4°C in a SW41 swinging-bucket rotor. After centrifugation, the fraction corresponding to the density of 1.13–1.19 g/mL (typically between the 1.16 M and 1.3 M sucrose layers) was carefully collected. This fraction was diluted with at least 5 volumes of PBS and subjected to a final ultracentrifugation at 100,000 ×g for 70 min at 4°C. The final pellet was resuspended in PBS for subsequent experiments. The protein concentration of the exosomes was determined using the Pierce BCA Protein Assay Kit (HYCEZMBIO, China). The isolated exosomes were either utilized in subsequent experimental procedures or cryopreserved at –80°C for future use. PMSC-Exos were characterized through transmission electron microscopy (TEM), nanoparticle tracking analysis (NTA), WB and nanoparticle flow cytometry (NanoFCM). TEM was used to assess vesicle morphology, while NTA measured size distribution and concentration. The presence of standard exosome-specific markers, including CD63, CD81, and TSG101, was verified by WB. Surface markers CD9 (NanoFCM, NHA009-A647-50T, 1:10), CD63 (NanoFCM, NHA063-A488-50T, 1:10) and CD81 (NanoFCM, NHA081-FITC-50T, 1:10) of exosomes were detected by NanoFCM (U30E, NanoFCM Inc, Xiamen,China).

Preparation of Protein Samples

PMSCs (three biological replicates, labeled PMSC1, PMSC2, and PMSC3) were cultured in 10 cm^2 dishes and treated with exosome-depleted medium for 48 hours. The cells and their conditioned media were harvested for further analysis. Exosome samples (Exos1, Exos2, and Exos3) were isolated from the culture supernatants of PMSC1, PMSC2, and PMSC3, respectively. Both cellular and exosomal fractions were processed for quantitative proteomic analysis using Tandem Mass Tag (TMT)-based labeling by Jingjie PTM BioLab (Hangzhou, China).

Protein extraction was performed by sonication on ice in a lysis buffer containing 8 M urea and 1% protease inhibitor cocktail. Proteins were precipitated with 15% trichloroacetic acid (TCA) at –20°C for 4 hours, then resolubilized in a buffer containing 8 M urea and 100 mM tetraethylammonium bromide (TEAB) at pH 8.0. Protein concentration was determined using the BCA assay kit (Boyotime, China). Reduction was achieved by incubating the samples with 5 mM

dithiothreitol (DTT) at 56°C for 30 minutes, followed by alkylation with 11 mM iodoacetamide for 15 minutes. To reduce the urea concentration to below 2 M, the samples were diluted with 100 mM TEAB. Trypsin was then introduced at a mass ratio of 1:50 (enzyme-to-protein) for digestion overnight, followed by a second digestion step at a 1:100 ratio for 4 h.

Tandem Mass Tag (TMT) Labeling and High Performance Liquid Chromatography (HPLC) Fractionation

Subsequent to digestion, the peptide underwent desalting via a Strata X C18 SPE column (Phenomenex) and was then subjected to vacuum drying. The peptide samples were reconstituted in 0.5 M TEAB and labeled with TMT reagents (Sigma, USA). TMT reagent was dissolved in acetonitrile and incubated with the peptide mixture at room temperature for 2 hours. After labeling, the peptides were combined, desalted, and dried by vacuum centrifugation.

Quantitative Proteomic Analysis by Liquid Chromatograph-Mass Spectrometer (LC-MS/MS)

The labeled peptides were solubilized in 0.1% formic acid (solvent A) and loaded onto a custom-made reversed-phase analytical column. A gradient elution was performed using solvent B (0.1% formic acid in 98% acetonitrile): the solvent concentration was increased from 6% to 23% over 26 minutes, from 23% to 35% over 8 minutes, and finally, to 80% over 3 minutes, holding at 80% for the last 3 minutes. The flow rate was maintained at 400 nL/min on an EASY-nLC 1000 UPLC system. The peptides were analyzed using tandem mass spectrometry (MS/MS) with an NSI source and a Q ExactiveTM Plus mass spectrometer (Thermo, USA). Electrospray ionization was applied at 2.0 kV, and the m/z range for data acquisition was set between 350 and 1800. Full scans were performed at a resolution of 70,000 in the Orbitrap, followed by MS/MS analysis of selected peptides with a normalized collision energy (NCE) of 28, and fragment ions were analyzed at a resolution of 17,500. The analysis alternated between a single MS scan and twenty MS/MS scans, with a dynamic exclusion of 15 seconds. The automatic gain control (AGC) target was set to 5E4, and the initial ion mass was set at 100 m/z.

Database Search and Bioinformatics Analysis

The MS/MS data were analyzed using the MaxQuant search engine (version 1.5.2.8), with the tandem mass spectra compared against the human UniProt database (https://www.uniprot.org/) and a reverse decoy database. Trypsin/P was used as the cleavage enzyme, allowing up to four missed cleavages. The mass tolerance for precursor ions was set at 20 ppm during the initial search and 5 ppm for the primary search, while fragment ion mass tolerance was 0.02 Da. Carbamidomethylation of cysteine was considered a fixed modification, and acetylation and oxidation of methionine were set as variable modifications. The false discovery rate (FDR) threshold was set at <1%, and a minimum peptide score of 40 was required for modified peptides. Differentially expressed proteins (DEPs) were identified based on an absolute fold change of ≥2 and a p-value < 0.05. Gene Ontology (GO) analysis was conducted to classify the identified proteins into three categories: cellular components, molecular functions, and biological processes, using the DAVID database (https://david.ncifcrf.gov/). Kyoto Encyclopedia of Genes and Genomes (KEGG) pathway enrichment analysis was performed using the clusterProfiler R package (version 3.18.0), with significance set at an adjusted p-value < 0.05. Furthermore, STRING (https://string-db.org/) was used to explore potential protein-protein interactions (PPI) involving THBS4, and the PPI network was constructed using the multi-protein online tool within the STRING database.

Western Blotting

Total proteins were extracted using RIPA buffer containing protease inhibitors and quantified using the BCA kit (Boyotime, China). Samples were separated by SDS-PAGE, transferred to polyvinylidene fluoride (PVDF) membranes (Millipore, Germany), and blocked with 5% skimmed milk in Tris-buffered saline containing 0.1% Tween-20 for 1 h. The catalogue numbers of the ladders are available in Supplementary Table 4. The antibody incubation and development were conducted in accordance with the manufacturer's guidelines. The primary antibodies used in this

research were CD63 (ab59479, Abcam, USA, mouse, 1:1000), CD81 (ab79559, Abcam, USA, mouse, 1:1000), Tsg101 (ab125011, Abcam, USA, rabbit, 1:5000), THBS4 (ab263898, Abcam, USA, rabbit, 1:1000), integrin α2 (ab181548, Abcam, USA, rabbit, 1:1000), p-AKT (Ser473, CST, USA, rabbit, 1:2000), AKT (C67E7, CST, USA, rabbit, 1:2000), β-Actin (66009-1-lg, Proteintech, China, mouse, 1:50,000), and GAPDH (60004-1-lg, Proteintech, China, mouse, 1:100,000). All the secondary antibodies (goat anti-rabbit and goat anti-mouse, 1:5000) were obtained from ABclonal Technology Co., Ltd. (Wuhan, China). The immunoreactive bands were visualized with an enhanced chemiluminescence reagent (Biosharp, China) and photographed using the ChemiDoc XRS+ system (Bio-Rad, USA). The unedited gels are available in Supplementary Figure 1.

RNA Isolation and Quantitative Real-Time PCR (RT-qPCR)

Total RNA was extracted using Trizol reagent (Vazyme, China). Reverse transcription was executed utilizing the HiScript Kit (Vazyme), followed by quantitative PCR employing the ChamQ SYBR Green PCR Kit (Vazyme) on LightCycler 480 equipment (Roche, Switzerland).

The relative gene expression was determined utilizing the $2^{-\Delta\Delta CT}$ technique. The primer sequences are enumerated in Supplementary Table 5.

Immunohistochemistry

Placental tissues were preserved using 4% paraformaldehyde. Paraffin embedding, paraffin sectioning, and immunohistochemical staining were conducted by Wuhan Pinuofei Biotechnology Co., Ltd. The primary antibodies utilized were CD31 (ab182981, Abcam, USA, rabbit, 1:4000) and THBS4 (sc-28293, Santa Cruz Biotechnology, USA, mouse, 1:200). Sections were examined utilising a light microscope (Olympus, Japan), and the results were analyzed employing ImageJ software.

Lentiviral Expression Constructs and Transfection

The lentiviruses carrying the THBS4 short hairpin RNA (shTHBS4) and negative control (shNC) sequences were acquired from Obio Technology (Shanghai, China). The shRNA lentivirus was then transfected into PMSCs with polybrene (5 μg/mL), and stable clones were selected using puromycin (5 μg/mL) (Biosharp, China). The shRNA sequences are listed in Supplementary Table 6.

Exosome Uptake Assay

PMSC-Exos were labelled with Dil dye (HYCEZMBIO, China) according to the manufacturer's instructions, then incubated with HUVECs for 24 h at 37°C. The cells were subsequently fixed with 4% paraformaldehyde and washed with PBS. After permeabilization with 0.5% Triton X-100, cells were subjected to staining with FITC-phalloidin and DAPI (Solarbio, China). Exosome internalisation was detected with a confocal laser scanning microscope (Olympus, Japan).

Transwell Migration Assay

Cell migration was detected using Transwell chambers (8.0 μm hole size; Corning, USA). Specifically, HUVECs (2.5×10^4 cells) were inoculated in the upper compartment with 200 μL of serum-free medium, whereas the lower chamber contained 700 μL of media enriched with 20% foetal bovine serum. Following 24 hours of incubation, migrating cells were fixed in 4% paraformaldehyde, stained with crystal violet, and visualized using an inverted microscope (Olympus, Japan). Cell counts were conducted in five randomly chosen fields per chamber at a magnification of 100×.

Tube Formation Assay

A 24-well plate was pre-coated with 50 μL of Matrigel (Corning, USA) and incubated at 37°C for 30 minutes to allow polymerization. HUVECs (2×10^4 cells/well) were inoculated in 200 μL of conditioned media and incubated for 8 h. The creation of capillary-like tubes was evaluated using a bright-field microscope at 100× magnification, and the total length

of the tubular structures was measured with ImageJ software. Three independent experiments were required for each treatment.

Immunofluorescence

Cells were fixed with 4% paraformaldehyde for 30 minutes at room temperature, followed by three washes with PBS. After blocking with 5% bovine serum albumin (BSA) for 1 hour, the cells were incubated overnight at 4°C with primary antibodies against THBS4 (sc-28293, Santa Cruz Biotechnology, USA, mouse) and integrin α2 (ab181548, Abcam, USA, rabbit). After washing with PBS, cells were incubated with species-specific fluorophore-conjugated secondary antibodies (Proteintech, China, 1:300) for one hour in the dark at ambient temperature. Nuclear counterstaining was conducted utilising DAPI (Solarbio, China). Fluorescent pictures were obtained via a laser confocal microscope (Olympus, Japan).

Plasmid Transfection

To induce ITG α2 overexpression, HUVECs were transfected with ITG α2 overexpression plasmids or corresponding negative control plasmids (Shanghai Genechem Co., Ltd., China) using Lipofectamine 3000 reagent (L3000–015, Thermo Fisher Scientific, Germany), in accordance with the manufacturer's instructions. The transfected cells were designated as OE-NC (negative control) and OE-ITG α2 (overexpression group) for downstream analyses.

Animals and Experimental Groups

All animal procedures received approval from the Animal Ethics Committee of Huazhong University of Science and Technology (approval number: 4076) and were conducted in compliance with National Institutes of Health (NIH) guidelines. Forty-five Sprague-Dawley (SD) rats, aged 8 to 10 weeks and weighing between 240 and 260 grammes, were procured from Hubei Biont Biological Technology Co., Ltd., and maintained in specified pathogen-free (SPF) conditions with unrestricted access to food and water. Female rats were paired with weight-matched males (2:1 ratio) overnight. The time scheme of the animal experiment is shown in a schematic diagram (Figure 1A). The presence of sperm or a vaginal plug, observed under a light microscope, was designated as gestational day 1 (GD1) (Figure 1B). Thirty pregnant rats were randomly allocated into five groups: healthy control (NC, n=6) and four experimental groups (n=24), including PE, PE+Exos, PE+shTHBS4-Exos, and PE+PBS. PE was induced by intraperitoneal injection of N-Nitro-L-arginine Methyl Ester (L-NAME; R015327; RHAWN, China), a nitric oxide synthase inhibitor, from GD10 to GD14, as previously described.[25] The NC group was administered an equal volume of sterile 0.9% saline solution. The PE+ Exos and PE+shTHBS4-Exos groups were then injected with (80 μg of exosomes in 20 μL PBS),[27,30] respectively, whereas the PE+PBS group received an equal dose of PBS on GD15. The injection site is shown in Figure 1C. On GD19, pregnant rats were anaesthetised with pentobarbital sodium, and foetal, placental, and kidney tissues were extracted via caesarean section. Foetal and placental weights were documented, placental tissues were obtained for Western blot analysis and immunohistochemistry, and kidney tissues were collected for HE staining.

Analysis of Blood Pressure and Urine Protein

Systolic blood pressure (SBP) was assessed non-invasively with a blood pressure apparatus (Kent Scientific, USA) on GD10, GD16, and GD19. Each rat was pre-warmed at 38°C for 10 minutes prior to measurement to ensure accurate results. Urinary protein concentrations were assessed in urine samples utilising CBB kits acquired from Nanjing Jiancheng Bioengineering Institute on GD9, GD15, and GD20. A rise in SBP >30 mmHg and elevated proteinuria were used to confirm successful PE model establishment.

Hematoxylin–Eosin (H&E) Staining

Kidney tissues were fixed in 4% paraformaldehyde, embedded in paraffin, and sectioned at a thickness of 5 μm. Sections underwent deparaffinization and rehydration, and were thereafter stained with haematoxylin and eosin (H&E). Stained slides were affixed with neutral balsam and sealed with coverslips. Renal histological alterations were assessed using a light microscope.

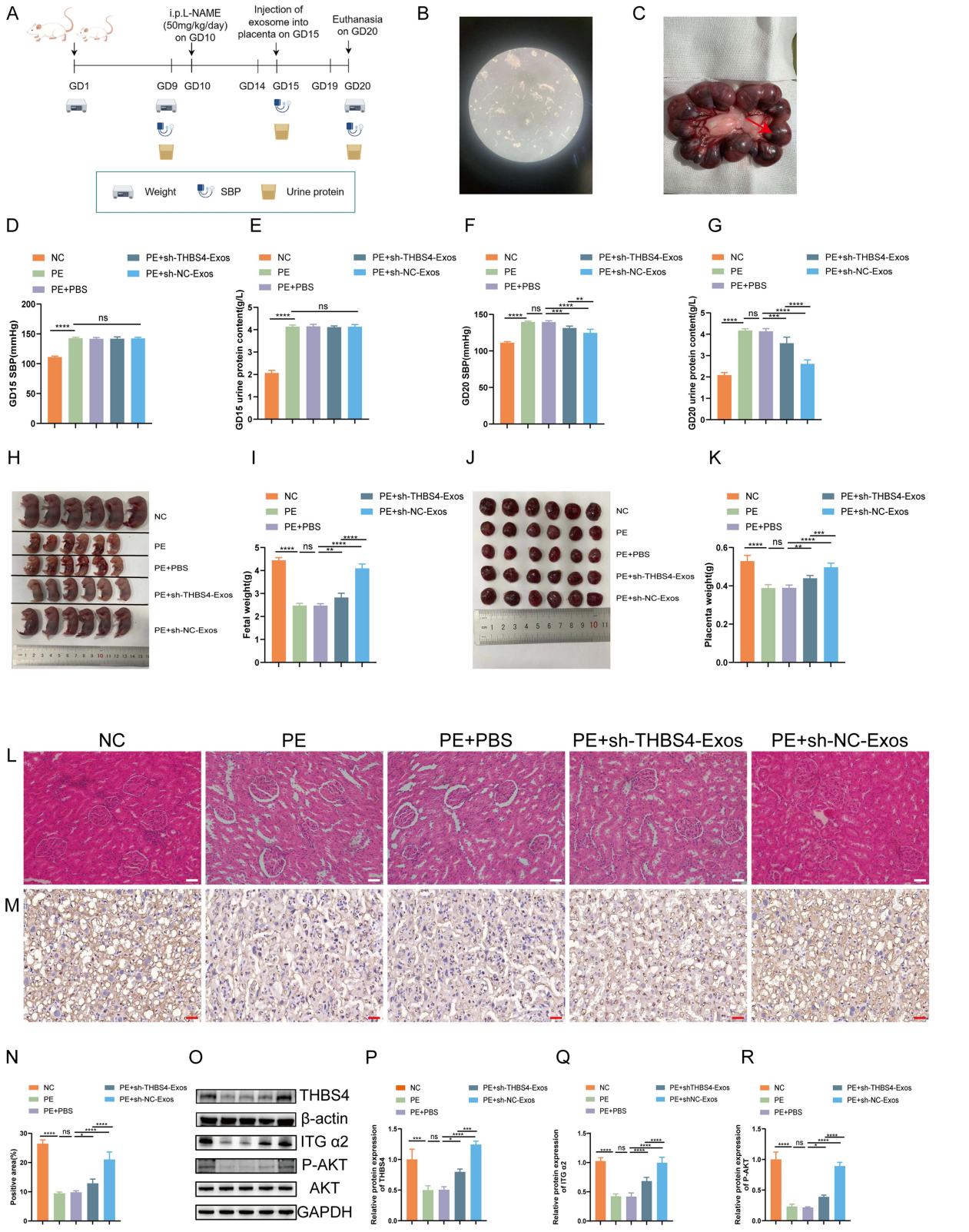

Figure 1 The therapeutic effect of THBS4-rich-PMSC-Exos in preeclamptic rats. (**A**) Schematic of our animal experiments. (**B**) Detection of sperm in vaginal smears on gestational day 1 (GD1) under a light microscope. (**C**) Location of placental injection (indicated by arrow). (**D** and **E**) Systolic blood pressure (SBP) measurements and urinary protein levels on GD15. (**F** and **G**) Systolic blood pressure (SBP) measurements and urinary protein levels on GD20. (**H** and **I**) Fetal morphology and weight on GD20 across various groups. (**J** and **K**) Placental morphology and weight on GD20 in different groups. (**L**) Representative HE staining of kidney sections showing pathological changes. Scale bar: 100 μm. (**M** and **N**) IHC staining of CD31 in placental tissues. Scale bar: 100 μm. (**O**–**R**) Analysis of THBS4, ITG α2, and phosphorylated AKT expression using Western blotting in each group. n=6. ns: no significance, **P*<0.05, ***P*<0.01, ****P*<0.001, *****P*<0.0001.

https://doi.org/10.2147/IJN.S572708

Statistical Analysis

All statistical analyses were performed using GraphPad Prism 8.0. Data are presented as the mean ± standard deviation from a minimum of three independent experiments. Comparisons between two groups were assessed using Student's *t*-test, whilst comparisons involving three or more groups were conducted using one-way ANOVA. A p-value of less than 0.05 was deemed statistically significant (*$P < 0.05$; **$P < 0.01$; ***$P < 0.001$; ****$P < 0.0001$).

Results

Isolation and Characterization of PMSC-Exos

Transmission electron microscopy demonstrated that the isolated exosomes displayed a characteristic spherical morphology with sizes between about 80 and 200 nm (Figure 2A). The whole section image for the microscopic image present in Figure 2A is available in Supplementary Figure 3. The size distribution of the isolated exosomes was evaluated using a Nanosight NS300. The particles in the device are reflected by the laser irradiation, leading to the observation of spots of varying sizes. The MODE curve showed a smooth and narrow peak, indicating a high level of purity. The peak particle size of 125 nm was consistent with the theoretical size of exosomes (Figure 2B). Western blot examination confirmed the presence of exosomal markers CD63, CD81, and TSG101 in PMSC-Exos, while these markers were diminished in parental PMSCs (Figure 2C). Flow cytometry analysis confirmed that the exosomes exhibited positive representative markers of CD9 (28.2%), CD63 (52.1%) and CD81 (54.2%) (Figure 2D). These findings collectively confirmed the successful isolation and characterization of PMSC-Exos.

The THBS4 Level is Upregulated in PMSC-Exos

We conducted proteomic analysis to examine the differential protein expression profiles between PMSC-Exos and PMSCs. With a threshold of an absolute fold change >2 and *p*-value <0.05, we identified 1,265 differentially expressed proteins, including 1080 up-expressed (PMSC-Exos-rich proteins) and 1105 down-expressed proteins (PMSCs-rich proteins) in PMSC-Exos, compared to PMSCs (Figure 3A). Furthermore, the subcellular localization analysis of the

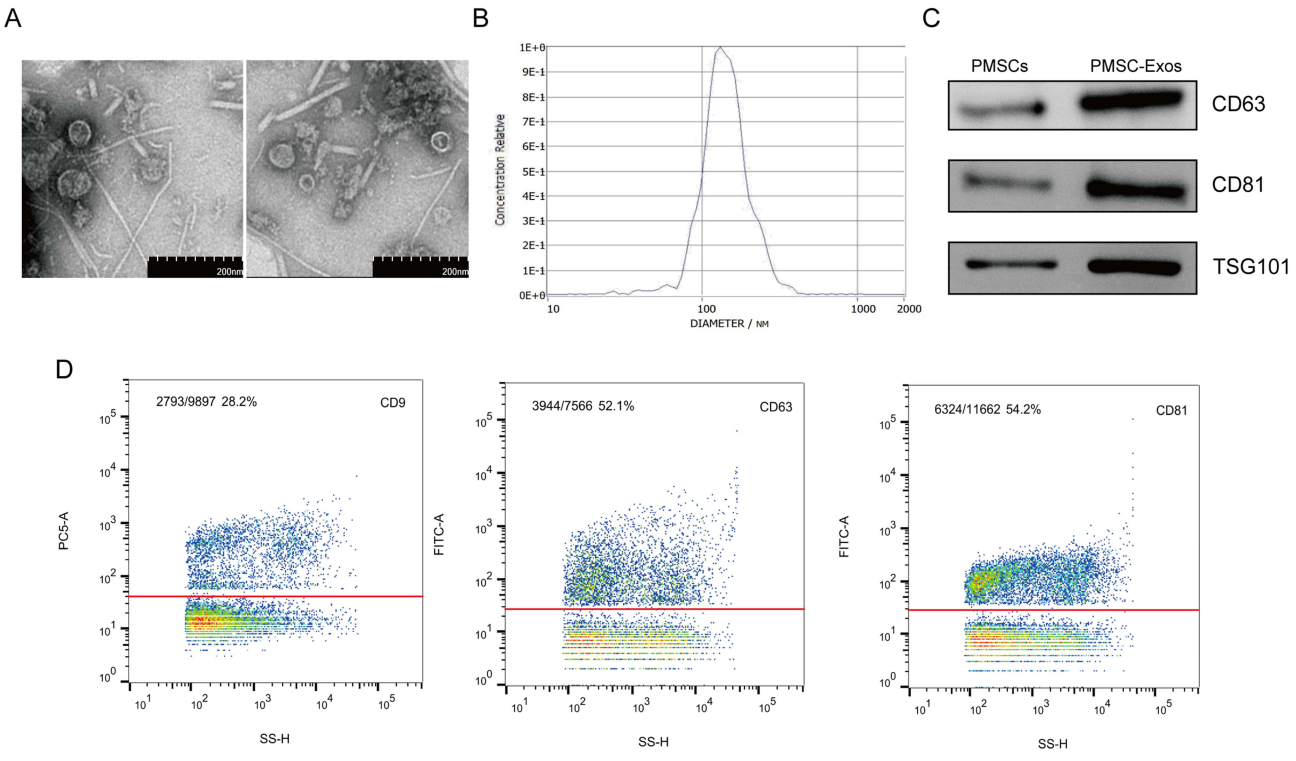

Figure 2 The identification of PMSC-Exos. (**A**) TEM image illustrating the characteristic shape of PMSC-Exos. Scale bar: 200 nm. (**B**) NTA showing the size distribution of PMSC-Exos. (**C**) Western blot analysis confirming the expression of exosomal surface markers CD63, CD81, and TSG101. (**D**) Exosome representative markers CD9, CD63, and CD81 were detected by flow cytometry analysis. n=3.

https://doi.org/10.2147/IJN.S572708

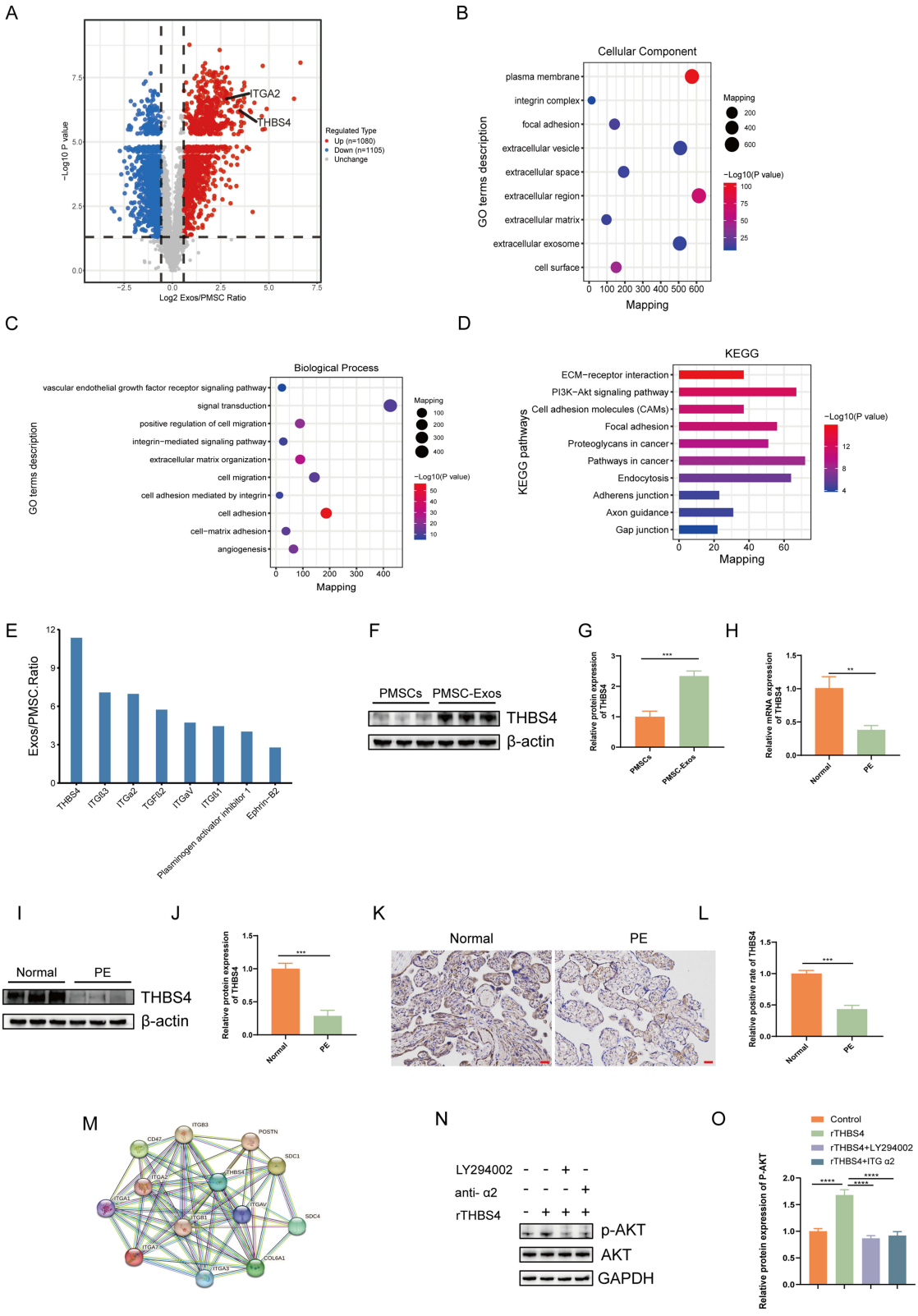

Figure 3 Proteomic profiling of PMSCs and PMSC-Exos. (**A**) Volcano plot showing differentially expressed proteins in PMSC-Exos compared to PMSCs. (**B**) GO analysis of upregulated proteins in terms of cellular component. (**C**) GO analysis of upregulated proteins in terms of biological processes. (**D**) KEGG pathway enrichment analysis of upregulated proteins. (**E**) Relative expression levels of angiogenesis-related proteins in PMSC-Exos versus PMSCs. (**F** and **G**) Western blotting analysis of THBS4 expression in PMSCs and PMSC-Exos. (**H**) THBS4 mRNA expression determined by RT-qPCR. (**I** and **J**) Western blotting analysis of THBS4 expression in normal and PE placenta. (**K** and **L**) IHC staining of THBS4 in placental tissues. Scale bar: 100 μm. (**M**) Predicted protein-protein interactions of THBS4. (**N** and **O**) Western blotting analysis of phosphorylated AKT in HUVECs under different treatment conditions. n=3. n=10 (H-K), ***P*<0.01, ****P*<0.001, *****P*<0.0001.

https://doi.org/10.2147/IJN.S572708

DEPs indicated that the elevated proteins in PMSC-Exos were predominantly located in the extracellular region, plasma membrane, extracellular exosome, and extracellular vesicle, a distinct distribution model (Figure 3B). Cluster analysis indicated that these proteins were mostly engaged in signal transduction, cell adhesion, angiogenesis, and cell migration (Figure 3C). KEGG pathway analysis indicated that the upregulated proteins were predominantly associated with cancer pathways and the PI3K-AKT signaling pathway (Figure 3D). The main upregulated angiogenesis-related proteins are shown in Figure 3E. Among them, THBS4 was the most significantly and differentially expressed of these proteins. We subsequently observed that THBS4 protein expression in PMSC-Exos was greatly elevated compared to that in PMSCs (Figure 3F and G). We quantified THBS4 mRNA expression levels in placental tissue samples from healthy individuals and those with preeclampsia using RT-qPCR. The findings indicated that THBS4 mRNA levels were markedly lower in PE (Figure 3H). The results from WB and IHC indicated that the expression of the THBS4 protein displayed a similar pattern (Figure 3I–L). Notably, THBS4 levels were similarly reduced in both early-onset and late-onset PE, and further analysis revealed no statistically significant difference in its expression between these two clinical subgroups (Supplementary Figure 3). Figure 3M illustrates the protein-protein interaction network of THBS4, as identified through the STRING database, which is mostly associated with integrins. Furthermore, recombinant THBS4 (rTHBS4) administration augmented AKT phosphorylation in HUVECs, a result that was diminished when co-administered with an integrin α2-specific blocking antibody or the PI3K inhibitor LY294002 (Figure 3N and O). These results suggest that THBS4 may exert its function via the ITG α2/PI3K/AKT axis.

Exosomal THBS4 Derived from PMSCs Promotes Migration and Angiogenesis of Human Umbilical Vein Endothelial Cells (HUVECs)

To explore the biological functions of THBS4 in PMSC-Exos on HUVECs, we successfully established lentiviral vectors (sh-THBS4 and sh-NC) and performed THBS4 knockdown in PMSCs (Figure 4A). Real-time PCR (Figure 4B) and Western blotting (Figure 4C and D) revealed a considerable reduction in THBS4 expression. Exosomes were then isolated from the supernatants of these transduced cells, and the expression of THBS4 was lower in endothelial cells treated with sh-THBS4-Exos compared to those treated with sh-NC-Exos (Figure 4E and F). Confocal microscopy demonstrated effective absorption of Dil-labeled PMSC-Exos by HUVECs (Figure 4G). Tube formation assay (Figure 4H and I) and transwell assay (Figure 4J and K) showed that HUVECs exhibited a much stronger migratory and angiogenic capacity when exposed to PMSC-Exos. Furthermore, the Transwell assay and tube formation assays revealed the significantly enhanced tube formation and migration of HUVECs, whereas these effects were markedly diminished when THBS4 was knocked down in the parental cells. Notably, treatment with rTHBS4 partially rescued the angiogenic and migratory deficits caused by THBS4 depletion. Furthermore, WB results revealed that the AKT phosphorylation protein expression showed a similar trend (Figure 4L and M).

Integrin α2 Mediates the Effects of THBS4-Induced in HUVECs

Integrin α2 has been identified as a THBS4 receptor, playing a key role in regulating endothelial cell migration and angiogenesis.[31,32] To investigate this, co-localization of THBS4 and integrin α2 was demonstrated on the surface of HUVECs by immunofluorescence staining (Figure 5A and B). Following rTHBS4 treatment (10 ng/mL, 48 h),[32] Western blotting revealed an upregulation of integrin α2 expression in HUVECs (Figure 5C and D). Furthermore, application of an α2-specific antibody attenuated THBS4-induced tube formation (Figure 5E and F) and migration (Figure 5G and H) capacities as well as AKT phosphorylation (Figure 5I and J) of HUVECs, confirming the pivotal role of integrin α2 in THBS4 signaling. Moreover, overexpression of ITGα2 in HUVECs (Figure 5K and L) reversed the inhibitory effects of sh-THBS4-Exos on angiogenesis (Figure 5M and N), migration (Figure 5O and P), and AKT phosphorylation of HUVECs (Figure 5Q and R), underscoring the functional relevance of the THBS4/ITGα2 axis.

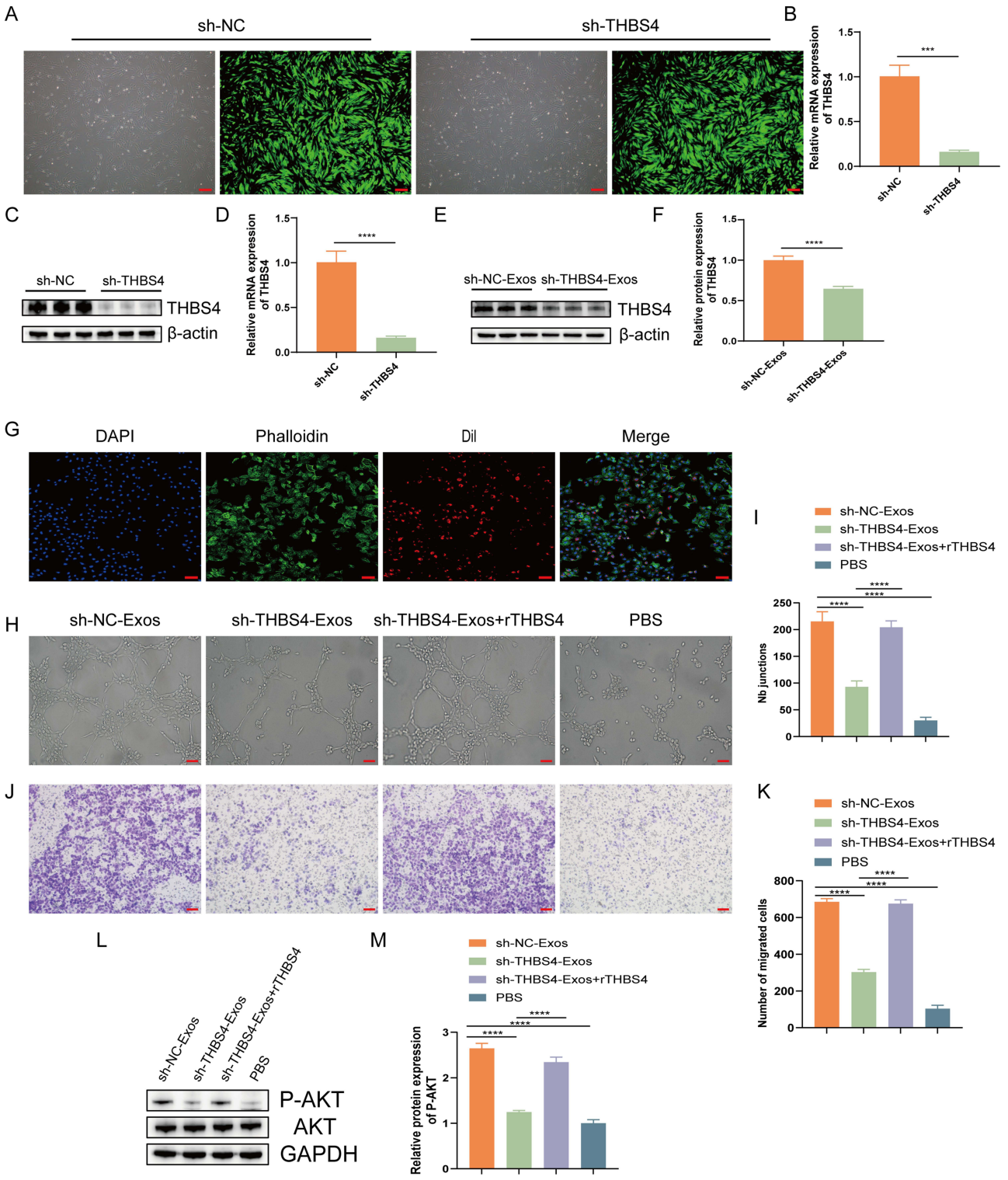

Figure 4 THBS4 mediates the pro-angiogenic and pro-migratory effects of PMSC-Exos on endothelial cells. (**A**) Lentiviral transfection of PMSCs with THBS4 shRNA or control vectors. Scale bar: 100 μm. (**B**–**D**) qRT-PCR and Western blotting analysis confirming THBS4 knockdown efficiency in PMSCs. (**E** and **F**) Western blotting analysis of THBS4 expression in exosomes derived from shNC- and shTHBS4-transfected PMSCs. (**G**) Confocal microscopy showing DiI-labeled exosome uptake by HUVECs. Scale bar: 100 μm. (**H** and **I**) Tube formation assays assessing angiogenesis of HUVECs under different treatments. Scale bar: 100 μm. (**J** and **K**) Transwell assays evaluating HUVEC migration under different treatments. Scale bar: 200 μm. (**L** and **M**) Western blot analysis of phosphorylated AKT levels in HUVECs after indicated treatments. n=3. ***P<0.001, ****P<0.0001.

https://doi.org/10.2147/IJN.S572708

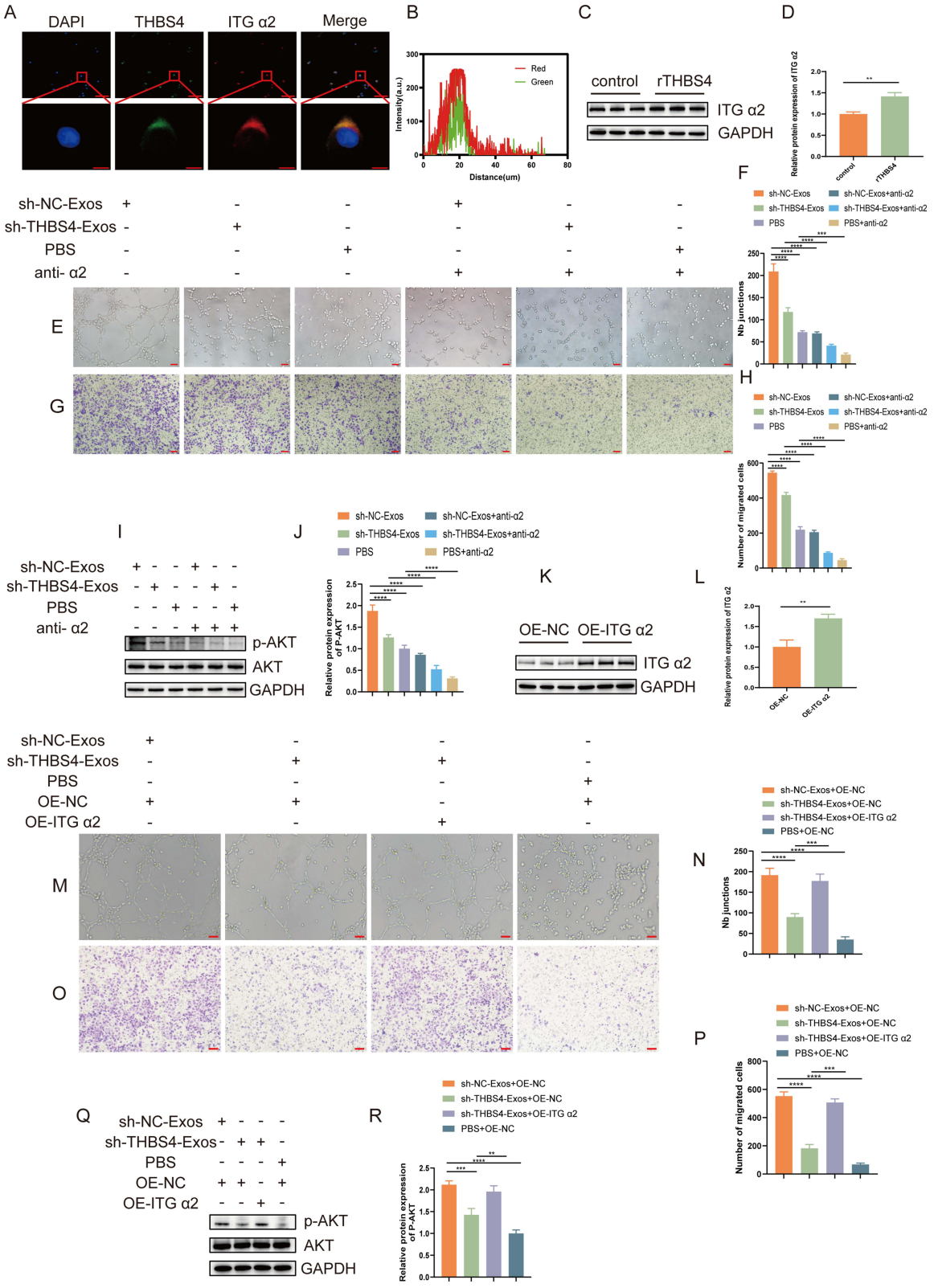

Figure 5 Integrin α2 mediates THBS4-induced migration, angiogenesis, and AKT phosphorylation in HUVECs. (**A** and **B**) immunofluorescence co-localization of THBS4 and integrin α2. Scale bars: 100 μm and 10 μm. (**C** and **D**) Western blotting analysis of integrin α2 expression. (**E** and **F**) Representative images of tube formation assays in HUVECs after various treatments. Scale bar: 100 μm. (**G** and **H**) Representative images of the migration assay after different treatments in HUVECs. Scale bar: 200 μm. (**I** and **J**) Western blotting analysis of AKT phosphorylation expression after different treatments in HUVECs. (**K** and **L**) integrin α2 protein expression in HUVECs. (**M** and **N**) Images of tubular structures formed by HUVECs in each treatment group. (Scale bar: 100 μm). (**O** and **P**) Images of migrated HUVECs in each group. Scale bar: 200 μm. (**Q** and **R**) Western blotting analysis of the expression of AKT phosphorylation in each group. n=3. ***P*<0.01, ****P*<0.001, *****P*<0.0001.

https://doi.org/10.2147/IJN.S572708

Inhibition of the PI3K/AKT Pathway effectively Prevents THBS4/Integrin α2 Axis-Induced Promotion of Angiogenesis and Migration

We examined the function of the PI3K/AKT pathway in mediating THBS4/ITGα2-induced cellular activities. The administration of the PI3K inhibitor LY294002 effectively abrogated THBS4/ITGα2-mediated tube formation (Figure 6A and B), migration (Figure 6C and D), and AKT phosphorylation (Figure 6E and F) in HUVECs, indicating that the PI3K/AKT pathway is a crucial downstream effector of the THBS4-integrin α2 axis.

Exosomal THBS4 Derived from PMSCs Ameliorated Systemic Symptoms and Safeguarded the Placentas and Foetuses From PE in vivo

A rat model of PE was constructed to assess the therapeutic potential of exosomal THBS4 in vivo. Compared to controls, PE rats exhibited significantly elevated systolic blood pressure (Figure 1D) and increased urinary protein excretion (Figure 1E). We conducted animal experiments with dose gradients to demonstrate the rationality of our dosage selection. According to relevant references, PMSC-Exos were administered at two distinct concentrations: a lower dose (40 μg of exosomal protein suspended in 20 μL PBS) and a higher dose (80 μg of exosomal protein in 20 μL PBS).[27,30] The results confirmed that treatment with PMSC-Exos ameliorated clinical symptoms and improved pregnancy outcomes in the PE rat model in a clear, dose-dependent manner, with the high-dose group (80 μg of exosomal protein in 20 μL PBS) showing significantly more pronounced therapeutic effects (Supplementary Figure 4). Based on these results, we selected the higher dose (80 μg of exosomes in 20 μL PBS) for subsequent mechanistic studies.

Notably, administration of PMSC-Exos lowered SBP and proteinuria levels (Figure 1F and G). PE-induced reductions in fetal (Figure 1H and I) and placental weight (Figure 1J and K). Histological examination by H&E staining showed that PMSC-Exos ameliorated renal damage characterized by glomerular atrophy and tubular dilation (Figure 1L). IHC revealed that the placentas of PE rats had much lower expression of CD31, which is a marker of angiogenesis,[33] than the PMSC-Exos group (Figure 1M and N). Western blotting revealed that THBS4, ITG α2, and phosphorylated AKT levels were decreased in PE placentas and were markedly upregulated after PMSC-Exo administration (Figure 1O–R). Importantly, in all animal experiments, the beneficial effects of PMSC-Exos were diminished upon THBS4 knockdown in the exosomes, further confirming the central role of THBS4 in mediating therapeutic efficacy.

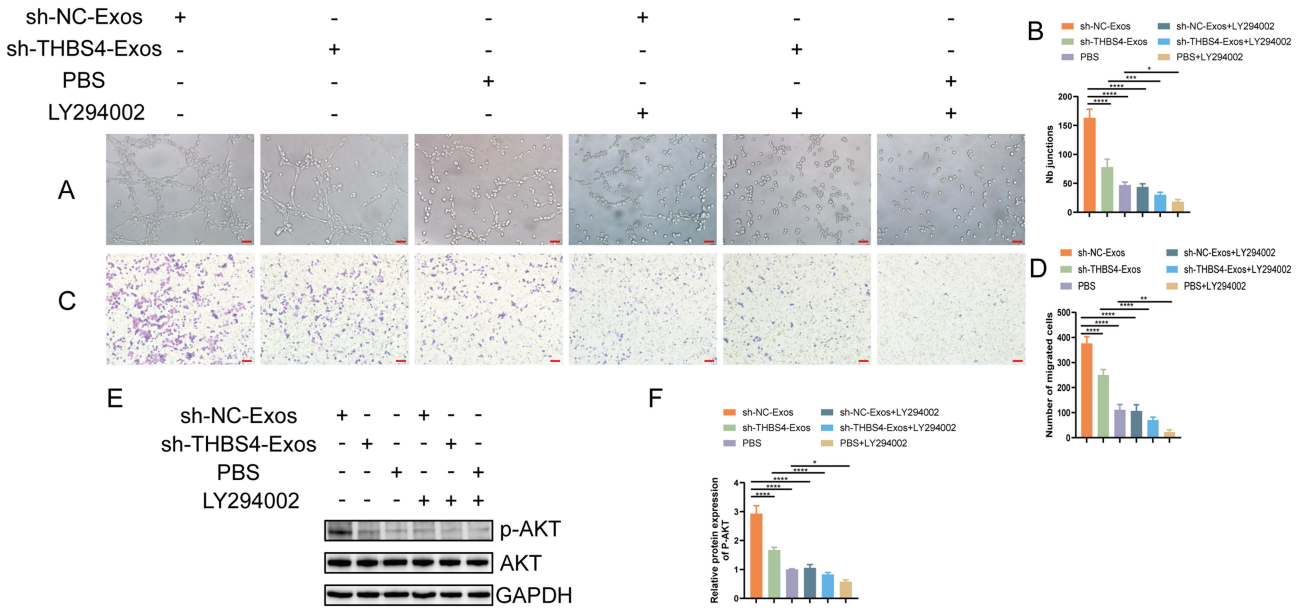

Figure 6 The inhibition of the PI3K/AKT pathway counteracts the angiogenic and migratory enhancement mediated by THBS4/integrin α2. (**A** and **B**) Representative tube formation images of HUVECs under indicated treatments. Scale bar: 100 μm. (**C** and **D**) Representative pictures of migrated HUVECs from transwell assays. Scale bar: 200 μm. (**E** and **F**) Western blotting analysis of the expression of AKT phosphorylation in each group. n=3. **P*<0.05, ***P*<0.01, ****P*<0.001, *****P*<0.0001.

https://doi.org/10.2147/IJN.S572708

Discussions

PE is a highly common pregnancy-specific syndrome and a primary cause of maternal mortality. Despite extensive research, effective treatments are limited.[4] Vascular endothelial dysfunction is widely recognized as a central pathophysiological mechanism of PE, contributing to impaired placental perfusion, increased vascular permeability, and systemic maternal symptoms.[34] Our research indicated that PMSC-Exosomes markedly improved the angiogenic and migratory abilities of HUVECs. A proteomic study indicated that PMSC-Exos are abundant in proteins associated with angiogenesis and cell migration, particularly the pro-angiogenic protein thrombospondin-4 (THBS4), which exhibited markedly high expression levels. Subsequent investigations demonstrated that THBS4 was crucial for the enhancement of angiogenic and migratory responses in endothelial cells produced by PMSC-Exos through the ITG α2/PI3K/AKT pathway. Topical PMSC-Exos therapy enhanced pregnancy outcomes in preeclamptic rats. However, these effects were markedly attenuated by inhibiting THBS4 expression in PMSC-Exos. Our results suggest that PMSC-Exos may transfer THBS4 protein to resident endothelial cells, thereby promoting their migratory and angiogenic abilities, accelerating revascularization, and alleviating the process of preeclampsia.

THBS4 is an extracellular matrix glycoprotein regulating cell-cell and cell-matrix interaction.[31] It belongs to the platelet-responsive protein family, consisting of five highly homologous members (THBS1, THBS2, THBS3, THBS4, and THBS5).[35] Extensive research indicates that THBS4 is a multifunctional protein integral to angiogenesis,[32,36] wound healing,[37] inflammation,[38] cardiovascular function,[39] cancer progression,[40–43] and so on. One study revealed that THBS4 has pro-angiogenic activity, and the proliferation and migration of endothelial cells were significantly inhibited in THBS4 knockout mice, whereas recombinant THBS4 promoted endothelial cell proliferation and migration functions.[36] Another study demonstrated that THBS4-modified bone marrow mesenchymal stromal cells have been shown to promote angiogenesis in a severe limb ischemia model in diabetic rats.[44] Collectively, these findings indicate that THBS4 may enhance placental vascularization and hence ameliorate preeclampsia. In accordance with these findings, our work demonstrated a considerable increase in THBS4 expression in PMSC-Exos, and the reduction of THBS4 in PMSCs diminished the capacity of their exosomes to enhance endothelial cell migration and tube formation. Furthermore, the addition of exogenous rTHBS4 rescued this inhibitory effect, supporting its essential role in exosome-mediated endothelial activation. In vivo, PMSC-Exos ameliorated PE-related symptoms and improved pregnancy outcomes in a preeclamptic rat model, while inhibition of THBS4 expression in exosomes markedly attenuated these protective effects. Furthermore, we demonstrated that the expression of THBS4 is downregulated in preeclamptic placental tissues compared with normal controls. Taken together, THBS4 may serve as a key molecule in vascular development and the improvement of endothelial dysfunction, and a critical therapeutic target for preeclampsia.

Studies have identified several potential receptors for THBS4, including integrins (ITGαMβ2, ITGα2β1, ITGαvβ3, ITGαvβ5), α2δ-1 (gabapentin receptor), and heparan sulfate receptors. Among these, endothelial cells express ITGα2β1, ITGαvβ3, and ITGαvβ5.[31] Previous evidence indicates that ITGαvβ3 does not significantly contribute to endothelial migration, and ITGαvβ5 does not directly bind to THBS4.[45] In contrast, both protein-protein interaction predictions and direct experimental data consistently identify integrin α2 as a high-affinity receptor for THBS4 on endothelial cells, with this interaction functionally linked to migration and angiogenesis.[32,42,45,46] In endothelial migration, integrin α2 mediates adhesion to collagen and laminin within the basement membrane, linking the extracellular matrix to the cytoskeleton via talin and vinculin. Moderate integrin α2 activity supports directed endothelial migration during vessel sprouting. In angiogenesis, integrin α2 promotes neovascularization by enhancing endothelial adhesion and migration on collagen I, often facilitated by proteoglycans such as decorin.[47,48] Based on this evidence, we propose that integrin α2 serves as the primary receptor mediating THBS4-induced angiogenesis and migration in endothelial cells. Supporting this, our experiments demonstrate co-localization of THBS4 with integrin α2 on the surface of HUVECs. Functionally, treatment with recombinant THBS4 upregulated integrin α2 expression, while blocking integrin α2 with a specific antibody significantly inhibited THBS4-induced enhancements in endothelial cell migration, tube formation, and AKT phosphorylation. Together, these findings strongly suggest that THBS4 promotes endothelial function primarily through engagement and activation of the integrin α2 signaling pathway.

Furthermore, multiple studies have shown that the PI3K-AKT signaling pathway is a downstream effector of the THBS4/integrin α2 axis.[32,42] Our proteomic analysis revealed that PI3K-AKT signaling-related proteins were enriched in PMSC-Exos. In line with this, we found that PMSC-Exos-derived THBS4 effectively promoted phosphorylation of AKT, an indicator of PI3K pathway activation. Importantly, inhibition of PI3K with LY294002 markedly reduced the THBS4-induced migration, tube formation, and AKT phosphorylation in HUVECs. These findings indicate that AKT activation is essential for mediating the pro-angiogenic and pro-migratory effects of PMSC-Exos-derived THBS4. Taken together, our data support a mechanistic model in which THBS4 carried by PMSC-Exos binds to integrin α2 on endothelial cells, thereby activating the PI3K-AKT signaling pathway. This activation promotes endothelial cell migration and angiogenesis, contributing to vascular remodeling and the amelioration of preeclampsia-related endothelial dysfunction.

Finally, based on the elucidated mechanism, we explored the therapeutic potential of PMSC-Exos in vivo by performing local placental injections in a rat model of preeclampsia. Our results demonstrated that the upregulation of THBS4 in preeclamptic rats alleviated hallmark symptoms of the disease, including elevated systolic blood pressure, proteinuria, and histological evidence of placental and renal injury. Mechanistically, these improvements were mediated via activation of the integrin α2/AKT signaling axis. Previous studies have shown that knockdown of THBS4 by local administration of THBS4 shRNA in pregnant rats could induce preeclampsia-like clinical features.[26] In our current study, we observed a downregulation of THBS4 expression in the placentas of PE rats compared to controls. However, treatment with PMSC-Exos effectively restored THBS4 levels. Collectively, our study presents novel evidence that THBS4 is a crucial mediator in the pathogenesis of PE. The ability of PMSC-Exos to upregulate THBS4 and activate the ITG α2/AKT signaling cascade offers a promising therapeutic strategy for ameliorating placental dysfunction in PE. These findings not only deepen our comprehension of the molecular pathways associated with PE but also underscore the potential of targeting the THBS4 axis in the development of future therapeutic approaches.

Notably, THBS4 inhibition did not fully abrogate the angiogenic effects of PMSC-Exos, indicating the involvement of additional functional proteins. Our proteomics data revealed that other pro-angiogenic factors, including integrin αV, integrin β3, TGFβ2, and Ephrin-B2, were also enriched in PMSC-Exos. This suggests that the angiogenic effects of PMSC-Exos are likely mediated through a coordinated network of signaling molecules, rather than a single dominant factor. These findings reflect the complexity and redundancy of the molecular mechanisms involved in vascular development and repair.

Despite the promising therapeutic potential of PMSC-Exos, certain limitations in our study must be acknowledged. First, the placenta local injection method, although effective in animal models, is invasive and may not be feasible in clinical settings. Future studies should explore less invasive delivery approaches and compare their therapeutic efficacy. Second, due to ethical constraints, our investigations were limited to rodent models, and the translational relevance to human PE remains to be verified. Extensive clinical trials are required to assess the safety, pharmacokinetics, and therapeutic effectiveness of PMSC-Exos in pregnant women with preeclampsia. Third, while we observed a downregulation of THBS4 in PE placentas, our clinical sample size, particularly when subdivided into early-onset (n=5) and late-onset (n=5) cases, was not sufficiently powered to conduct a robust comparative analysis between these clinically distinct subgroups. Future studies with larger, well-characterized cohorts are warranted to explore whether the role and regulation of THBS4 differ between early-onset preeclampsia and late-onset preeclampsia, which may have implications for targeted therapeutic strategies.

Conclusions

In this study, we identified that THBS4 levels are markedly increased in PMSC-Exos relative to PMSCs and are crucial in the management of PE. Our findings have demonstrated that THBS4-enriched PMSC-Exos enhance endothelial cell migration and angiogenesis via the integrin α2/PI3K/AKT signaling pathway in vitro and improve pregnancy outcomes in a preeclampsia-like rat model in vivo (Figure 7). These results uncover a novel regulatory mechanism underlying the therapeutic effects of PMSC-Exos in PE. Targeting the THBS4/integrin α2/PI3K/AKT axis may represent a promising strategy for the development of PE therapies. To advance this toward clinical translation, the efficacy and safety of PMSC-Exos require validation in more physiologically relevant models, such as primate models and human placental organoids.[49–51] Furthermore, our findings underscore the promise of THBS4-based interventions as a key future

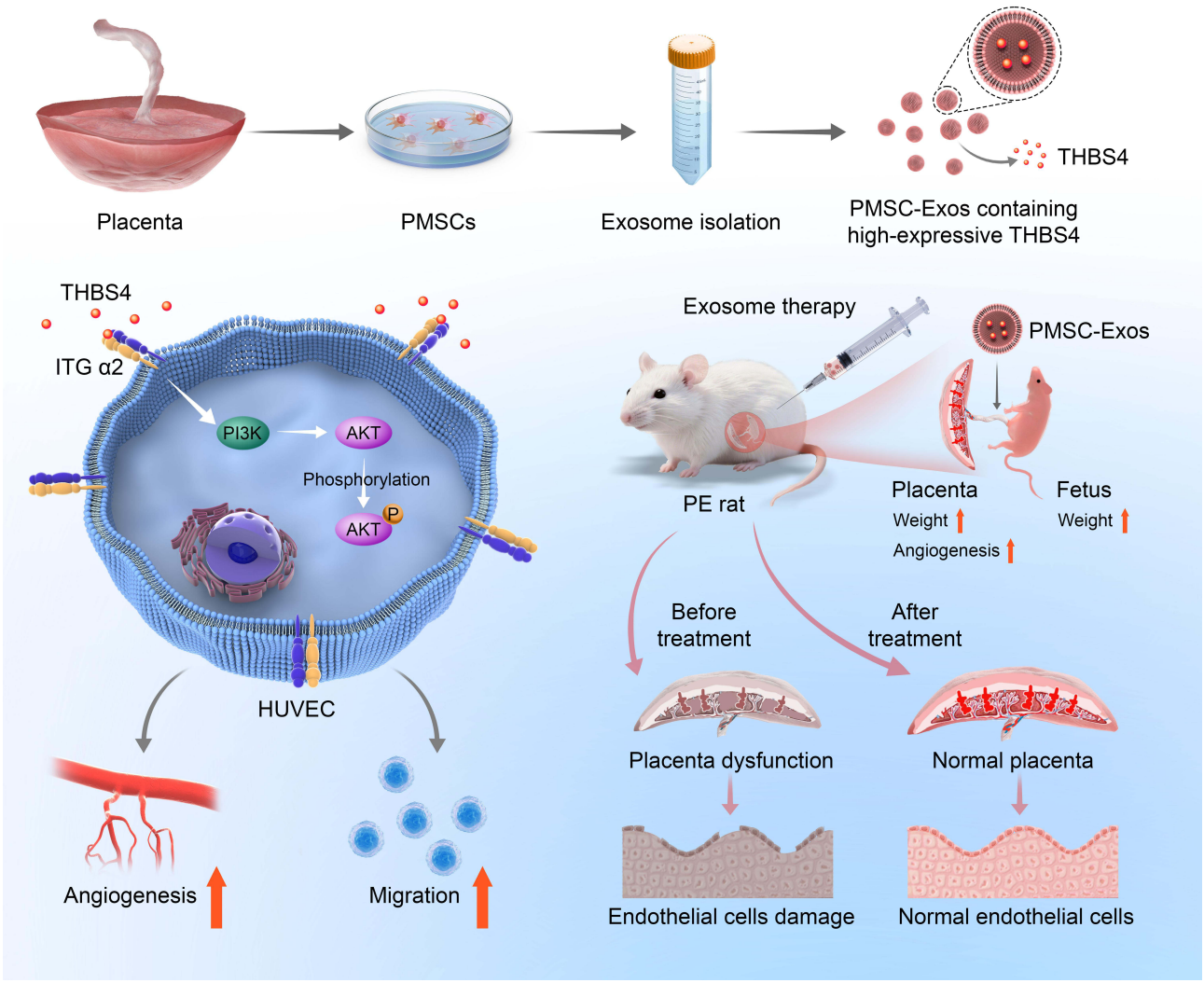

Figure 7 Schematic illustration of the proposed mechanism. PMSC-derived exosomes (PMSC-Exos) enhance angiogenesis and tube formation of HUVECs and improve pregnancy outcomes in preeclamptic rats through the THBS4/integrin α2 (ITGα2)/PI3K/AKT signaling axis. The upward-pointing arrow denotes an increase.
Abbreviations: PMSCs, Placental mesenchymal stem cells; PMSC-Exos, Placental mesenchymal stem cell exosomes; THBS4, Thrombospondin-4; ITG α2, Integrin α2; PI3K, Phosphatidylinositol 3-Kinase; AKT, Protein Kinase B; P-AKT, Phosphorylated Protein Kinase B; HUVEC, Human umbilical vein endothelial cell; PE, preeclampsia.

direction. Promising strategies to explore include the delivery of recombinant THBS4 protein—potentially encapsulated within biocompatible polymers like poly(lactide-co-glycolide) (PLGA) for sustained release[52]—to directly compensate for its deficiency, as well as the use of exosomes genetically engineered to overexpress THBS4 to enhance therapeutic effects.[53]

Abbreviations

PE, Preeclampsia; PMSCs, Placental mesenchymal stem cells; MSC-Exos, Mesenchymal stem cell exosomes; PMSC-Exos, Placental mesenchymal stem cell exosomes; TEM, Transmission electron microscopy; NTA, Nanoparticle tracking analysis; NanoFCM, nanoparticle flow cytometry; THBS4, Thrombospondin-4; WB, Western blotting; IHC, Immunohistochemistry; HUVECs, Human umbilical vein endothelial cells; H&E, Hematoxylin and eosin; ITG, Integrin; MSCs, Mesenchymal stem cells; Exos, Exosomes; HO-1, Heme oxygenase-1; ECM, Endothelial cell medium; PBS, Phosphate-buffered saline; TEAB, Tetraethylammonium bromide; TMT, Tandem Mass Tag; HPLC, High Performance Liquid Chromatography; DEPs, Differentially expressed proteins; GO, gene ontology; KEGG, Kyoto Encyclopedia of Genes and Genomes; PPI, Protein-protein interaction; PVDF, Polyvinylidene fluoride; BSA, Bovine

serum albumin; SD, Sprague–Dawley; SPF, Specific pathogen-free; GD, Gestational day; L-NAME, N-Nitro-L-arginine Methyl Ester; SBP, Systolic blood pressure; rTHBS4, Recombinant THBS4.

Data Sharing Statement

The datasets generated and analyzed during the current study are available from the corresponding author on reasonable request.

Ethics Statement

This study was approved by the Ethical Committee of Wuhan Union Hospital, affiliated with Huazhong University of Science and Technology. Written informed consent was obtained from all patients who agreed to participate in the study. Sample collection was carried out in accordance with the Declaration of Helsinki. All animal experiments were approved by the Ethics Committee of Wuhan Union Hospital and were conducted following China's Guidelines for the Ethical Review of Laboratory Animal Welfare (GBT 35892–2018). We confirm that all methods were performed in compliance with the relevant guidelines and regulations, as stated in the Ethics Approval and Consent to Participate section.

Author Contributions

All authors made a significant contribution to the work reported, whether that is in the conception, study design, execution, acquisition of data, analysis and interpretation, or in all these areas; took part in drafting, revising or critically reviewing the article; gave final approval of the version to be published; have agreed on the journal to which the article has been submitted; and agree to be accountable for all aspects of the work.

Funding

This work was supported by the National Natural Science Foundation of China (Grant number: 82171678), the Shenzhen Science and Technology Program (Grant number: JCYJ20230807143504009), and the Science, Technology, and Innovation Commission of Shenzhen Municipality (Grant number: JCYJ20200109140614667).

Disclosure

The authors report no conflicts of interest in this work.

References

1. Rana S, Lemoine E, Granger JP, Karumanchi SA. Preeclampsia: pathophysiology, Challenges, and Perspectives. *Circ Res*. 2019;124(7):1094–1112. doi:10.1161/CIRCRESAHA.118.313276
2. Phipps EA, Thadhani R, Benzing T, Karumanchi SA. Pre-eclampsia: pathogenesis, novel diagnostics and therapies. *Nat Rev Nephrol*. 2019;15(5):275–289. doi:10.1038/s41581-019-0119-6
3. Kariori M, Katsi V, Tsioufis C. Late vs. Early Preeclampsia. *Int J Mol Sci*. 2025;26(22):11091. doi:10.3390/ijms262211091
4. Dimitriadis E, Rolnik DL, Zhou W, et al. Pre-eclampsia. *Nat Rev Dis. Primers*. 2023;9(1):8. doi:10.1038/s41572-023-00417-6
5. Murthi P, Pinar AA, Dimitriadis E, Samuel CS. Inflammasomes-A Molecular Link for Altered Immunoregulation and Inflammation Mediated Vascular Dysfunction in Preeclampsia. *Int J Mol Sci*. 2020;21(4):1406. doi:10.3390/ijms21041406
6. Lan T, Luo M, Wei X. Mesenchymal stem/stromal cells in cancer therapy. *J Hematol Oncol*. 2021;14(1):195. doi:10.1186/s13045-021-01208-w
7. Mei R, Wan Z, Yang C, et al. Advances and clinical challenges of mesenchymal stem cell therapy. *Front Immunol*. 2024;15:1421854. doi:10.3389/fimmu.2024.1421854
8. Lin Z, Wu Y, Xu Y, Li G, Li Z, Liu T. Mesenchymal stem cell-derived exosomes in cancer therapy resistance: recent advances and therapeutic potential. *Mol Cancer*. 2022;21(1):179. doi:10.1186/s12943-022-01650-5
9. Liu J, Gao J, Liang Z, et al. Mesenchymal stem cells and their microenvironment. *Stem Cell Res Ther*. 2022;13(1):429. doi:10.1186/s13287-022-02985-y
10. Shi H, Yang Z, Cui J, Tao H, Ma R, Zhao Y. Mesenchymal stem cell-derived exosomes: a promising alternative in the therapy of preeclampsia. *Stem Cell Res Ther*. 2024;15(1):30. doi:10.1186/s13287-024-03652-0
11. Koohsarian P, Talebi A, Rahnama MA, Zomorrod MS, Kaviani S, Jalili A. Reviewing the role of cardiac exosomes in myocardial repair at a glance. *Cell Biol Int*. 2021;45(7):1352–1363. doi:10.1002/cbin.11515
12. Tan F, Li X, Wang Z, Li J, Shahzad K, Zheng J. Clinical applications of stem cell-derived exosomes. *Signal Transduct Target Ther*. 2024;9(1):17. doi:10.1038/s41392-023-01704-0
13. Ahmed L, Al-Massri K. New Approaches for Enhancement of the Efficacy of Mesenchymal Stem Cell-Derived Exosomes in Cardiovascular Diseases. *Tissue Eng Regen Med*. 2022;19(6):1129–1146. doi:10.1007/s13770-022-00469-x

14. Jafarinia M, Alsahebfosoul F, Salehi H, Eskandari N, Ganjalikhani-Hakemi M. Mesenchymal Stem Cell-Derived Extracellular Vesicles: a Novel Cell-Free Therapy. *Immunol Invest*. 2020;49(7):758–780. doi:10.1080/08820139.2020.1712416
15. Jiang Y, Luo T, Xia Q, Tian J, Yang J. microRNA-140-5p from human umbilical cord mesenchymal stem cells–released exosomes suppresses preeclampsia development. *Funct Integr Genomics*. 2022;22(5):813–824. doi:10.1007/s10142-022-00848-6
16. Chen Y, Ding H, Wei M, et al. MSC-Secreted Exosomal H19 Promotes Trophoblast Cell Invasion and Migration by Downregulating let-7b and Upregulating FOXO1. *Mol Ther Nucleic Acids*. 2020;19:1237–1249. doi:10.1016/j.omtn.2019.11.031
17. Chang X, He Q, Wei M, et al. Human umbilical cord mesenchymal stem cell derived exosomes (HUCMSC-exos) recovery soluble fms-like tyrosine kinase-1 (sFlt-1)-induced endothelial dysfunction in preeclampsia. *Eur J Med Res*. 2023;28(1):277. doi:10.1186/s40001-023-01182-8
18. Pan Y, Wu W, Jiang X, Liu Y. Mesenchymal stem cell-derived exosomes in cardiovascular and cerebrovascular diseases: from mechanisms to therapy. *Biomed Pharmacother*. 2023;163:114817. doi:10.1016/j.biopha.2023.114817
19. Zargar MJ, Kaviani S, Vasei M, Soufi Zomorrod M, Heidari Keshel S, Soleimani M. Therapeutic role of mesenchymal stem cell-derived exosomes in respiratory disease. *Stem Cell Res Ther*. 2022;13(1):5. doi:10.1186/s13287-022-02866-4
20. Wang C, Zhou H, Wu R, et al. Mesenchymal stem cell-derived exosomes and non-coding RNAs: regulatory and therapeutic role in liver diseases. *Biomed Pharmacother*. 2023;157:114040. doi:10.1016/j.biopha.2022.114040
21. Clua-Ferré L, Suau R, Vañó-Segarra I, Ginés I, Serena C, Manyé J. Therapeutic potential of mesenchymal stem cell-derived extracellular vesicles: a focus on inflammatory bowel disease. *Clin Transl Med*. 2024;14(11):70075. doi:10.1002/ctm2.70075
22. Weng Z, Zhang B, Wu C, et al. Therapeutic roles of mesenchymal stem cell-derived extracellular vesicles in cancer. *J Hematol Oncol*. 2021;14 (1):1. doi:10.1186/s13045-021-01141-y
23. Zhao B, Wei J, Jiang Z, Long Y, Xu Y, Jiang B. Mesenchymal stem cell-derived exosomes: an emerging therapeutic strategy for hepatic ischemia-reperfusion injury. *Stem Cell Res Ther*. 2025;16(1):178. doi:10.1186/s13287-025-04302-9
24. Wu D, Liu Y, Liu Y, et al. Heme oxygenase-1 gene modified human placental mesenchymal stem cells promote placental angiogenesis and spiral artery remodeling by improving the balance of angiogenic factors in vitro. *Placenta*. 2020;99:70–77. doi:10.1016/j.placenta.2020.07.007
25. Liu Y, Shi H, Wu D, et al. The Protective Benefit of Heme Oxygenase-1 Gene-Modified Human Placenta-Derived Mesenchymal Stem Cells in a N-Nitro-L-Arginine Methyl Ester-Induced Preeclampsia-Like Rat Model: possible Implications for Placental Angiogenesis. *Stem Cells Dev*. 2021;30(19):174. doi:10.1089/scd.2021.0174
26. Shi H, Mao Y, Cui J, Ma R, Yang Z, Zhao Y. THBS4 downregulation alters trophoblast function in preeclampsia via the TGF-β1/Smad signaling cascade. *Am J Physiol Cell Physiol*. 2025;329(1):C170–C182. doi:10.1152/ajpcell.00387.2024
27. Chen Y, Jin J, Chen X, Xu J, An L, Ruan H. Exosomal microRNA-342-5p from human umbilical cord mesenchymal stem cells inhibits preeclampsia in rats. *Funct Integr Genomics*. 2023;23(1):27. doi:10.1007/s10142-022-00931-y
28. Haoran S, Zhishan J, Yan M, et al. Hypoxic Preconditioning Enhances Cellular Viability and Migratory Ability: role of DANCR/miR-656-3p/HIF-1α Axis in Placental Mesenchymal Stem Cells. *Stem Cells*. 2023;41(9):877–891. doi:10.1093/stmcls/sxad048
29. Zhu J, Liu B, Wang Z, et al. Exosomes from nicotine-stimulated macrophages accelerate atherosclerosis through miR-21-3p/PTEN-mediated VSMC migration and proliferation. *Theranostics*. 2019;9(23):6901–6919. doi:10.7150/thno.37357
30. Xiong Z-H, Wei J, Lu M-Q, Jin M-Y, Geng H-L. Protective effect of human umbilical cord mesenchymal stem cell exosomes on preserving the morphology and angiogenesis of placenta in rats with preeclampsia. *Biomed Pharmacothe*. 2018;105:1240–1247. doi:10.1016/j.biopha.2018.06.032
31. Stenina-Adognravi O, Plow EF. Thrombospondin-4 in tissue remodeling. *Matrix Biol*. 2019;75–76:300–313. doi:10.1016/j.matbio.2017.11.006
32. He L, Wang W, Shi H, et al. THBS4/integrin α2 axis mediates BM-MSCs to promote angiogenesis in gastric cancer associated with chronic Helicobacter pylori infection. *Aging*. 2021;13(15):19375–19396. doi:10.18632/aging.203334
33. Franz L, Alessandrini L, Calvanese L, Crosetta G, Frigo AC, Marioni G. Angiogenesis, programmed death ligand 1 (PD-L1) and immune microenvironment association in laryngeal carcinoma. *Pathology*. 2021;53(7):844–851. doi:10.1016/j.pathol.2021.02.007
34. Ives CW, Sinkey R, Rajapreyar I, Tita ATN, Oparil S. Preeclampsia-Pathophysiology and Clinical Presentations: JACC State-of-the-Art Review. *J Am Coll Cardiol*. 2020;76(14):1690–1702. doi:10.1016/j.jacc.2020.08.014
35. Chistiakov DA, Melnichenko AA, Myasoedova VA, Grechko AV. Thrombospondins: a Role in Cardiovascular Disease. *Int J Mol Sci*. 2017;18 (7):1540. doi:10.3390/ijms18071540
36. Muppala S, Xiao R, Krukovets I, et al. Thrombospondin-4 mediates TGF-β-induced angiogenesis. *Oncogene*. 2017;36(36):5189–5198. doi:10.1038/onc.2017.140
37. Klaas M, Mäemets-Allas K, Heinmäe E, et al. Thrombospondin-4 Is a Soluble Dermal Inflammatory Signal That Selectively Promotes Fibroblast Migration and Keratinocyte Proliferation for Skin Regeneration and Wound Healing. *Front Cell Dev Biol*. 2021;9:745637. doi:10.3389/fcell.2021.745637
38. Mäemets-Allas K, Klaas M, Cárdenas-León CG, Arak T, Kankuri E, Jaks V. Stimulation with THBS4 activates pathways that regulate proliferation, migration and inflammation in primary human keratinocytes. *Biochem Biophys Res Commun*. 2023;642:97–106. doi:10.1016/j.bbrc.2022.12.052
39. Meng XM, Pang QY, Zhou ZF, et al. Histone methyltransferase MLL4 protects against pressure overload-induced heart failure via a THBS4-mediated protection in ER stress. *Pharmacol Res*. 2024;205:107263. doi:10.1016/j.phrs.2024.107263
40. Guo D, Zhang D, Ren M, et al. THBS4 promotes HCC progression by regulating ITGB1 via FAK/PI3K/AKT pathway. *FASEB J*. 2020;34 (8):10668–10681. doi:10.1096/fj.202000043R
41. Chen X, Huang Y, Wang Y, Wu Q, Hong S, Huang Z. THBS4 predicts poor outcomes and promotes proliferation and metastasis in gastric cancer. *J Physiol Biochem*. 2019;75(1):117–123. doi:10.1007/s13105-019-00665-9
42. Hou Y, Li H, Huo W. THBS4 silencing regulates the cancer stem cell-like properties in prostate cancer via blocking the PI3K/Akt pathway. *Prostate*. 2020;80(10):753–763. doi:10.1002/pros.23989
43. Chou KY, Chang AC, Ho CY, et al. Thrombospondin-4 promotes bladder cancer cell migration and invasion via MMP2 production. *J Cell Mol Med*. 2021;25(13):6046–6055. doi:10.1111/jcmm.16463
44. Zhang Q, Wang T, Wu X, et al. Thrombospondin-4 (TSP4) gene-modified bone marrow stromal cells (BMSCs) promote the effect of therapeutic angiogenesis in critical limb ischemia (CLI) of diabetic rats. *Biochem Biophys Res Commun*. 2020;532(2):231–238. doi:10.1016/j.bbrc.2020.06.148
45. Muppala S, Frolova E, Xiao R, et al. Proangiogenic Properties of Thrombospondin-4. *Arterioscler Thromb Vasc Biol*. 2015;35(9):1975–1986. doi:10.1161/ATVBAHA.115.305912

46. Tang Y, Xu Z, Xu F, et al. B4GALNT1 promotes hepatocellular carcinoma stemness and progression via integrin α2β1-mediated FAK and AKT activation. *JHEP Rep*. 2023;5(12):100903. doi:10.1016/j.jhepr.2023.100903
47. Chastney MR, Kaivola J, Leppänen V-M, Ivaska J. The role and regulation of integrins in cell migration and invasion. *Nat Rev Mol Cell Biol*. 2024;26(2):147–167. doi:10.1038/s41580-024-00777-1
48. Adorno-Cruz V, Liu H. Regulation and functions of integrin α2 in cell adhesion and disease. *Genes Dis*. 2019;6(1):16–24. doi:10.1016/j.gendis.2018.12.003
49. Huang L, Tu Z, Wei L, et al. Generating Functional Multicellular Organoids from Human Placenta Villi. *Adv Sci*. 2023;10(26):e2301565. doi:10.1002/advs.202301565
50. Huang S, Zhang Y, Guo Y, et al. Constructing a Preeclampsia Organoid Model to Elucidate the Mechanism of Aspirin. *Hypertension*. 2025;82(9):e171–e185. doi:10.1161/HYPERTENSIONAHA.125.25342
51. Tarantal AF, Hartigan-O'Connor DJ, Noctor SC. Translational Utility of the Nonhuman Primate Model. *Biol Psychiatry Cogn Neurosci Neuroimaging*. 2022;7(5):491–497. doi:10.1016/j.bpsc.2022.03.001
52. Zhang C, Yang L, Wan F, et al. Quality by design thinking in the development of long-acting injectable PLGA/PLA-based microspheres for peptide and protein drug delivery. *Int J Pharm*. 2020;585:119441. doi:10.1016/j.ijpharm.2020.119441
53. Cui J, Yang Z, Ma R, et al. Placenta-targeted Treatment Strategies for Preeclampsia and Fetal Growth Restriction: an Opportunity and Major Challenge. *Stem Cell Rev Rep*. 2024;20(6):1501–1511. doi:10.1007/s12015-024-10739-x